

University of Groningen

Obtaining stable solutions of the optimized-effective-potential method in the basis set representation

Fernandez, Julio J.; Kollmar, Christian; Filatov, Michael

Published in:
Physical Review A

DOI:
[10.1103/PhysRevA.82.022508](https://doi.org/10.1103/PhysRevA.82.022508)

IMPORTANT NOTE: You are advised to consult the publisher's version (publisher's PDF) if you wish to cite from it. Please check the document version below.

Document Version
Publisher's PDF, also known as Version of record

Publication date:
2010

[Link to publication in University of Groningen/UMCG research database](#)

Citation for published version (APA):

Fernandez, J. J., Kollmar, C., & Filatov, M. (2010). Obtaining stable solutions of the optimized-effective-potential method in the basis set representation. *Physical Review A*, 82(2), 022508-1-022508-6. [022508].
DOI: 10.1103/PhysRevA.82.022508

Copyright

Other than for strictly personal use, it is not permitted to download or to forward/distribute the text or part of it without the consent of the author(s) and/or copyright holder(s), unless the work is under an open content license (like Creative Commons).

Take-down policy

If you believe that this document breaches copyright please contact us providing details, and we will remove access to the work immediately and investigate your claim.

Downloaded from the University of Groningen/UMCG research database (Pure): <http://www.rug.nl/research/portal>. For technical reasons the number of authors shown on this cover page is limited to 10 maximum.

Obtaining stable solutions of the optimized-effective-potential method in the basis set representation

Julio J. Fernandez

Departamento de Física Fundamental, UNED, Apartado 60.141, E-28080 Madrid, Spain

Christian Kollmar

Institut für Physikalische und Theoretische Chemie, Universität Bonn, Wegelerstrasse 12, D-53115 Bonn, Germany

Michael Filatov*

University of Groningen, Nijenborgh 4, NL-9747AG Groningen, The Netherlands

(Received 6 November 2009; published 12 August 2010)

Equations of the optimized-effective-potential method in a basis set representation are solved with the use of the incomplete Cholesky decomposition technique. The resulting local potential is expanded in terms of the products of occupied and virtual Kohn-Sham orbitals thus avoiding the use of auxiliary basis sets. It is demonstrated that, for a sufficiently large orbital basis set satisfying the condition of linear dependence of these products, stable and numerically accurate solutions of the OEP method can be obtained with the use of the suggested computational approach.

DOI: [10.1103/PhysRevA.82.022508](https://doi.org/10.1103/PhysRevA.82.022508)

PACS number(s): 31.15.eg, 31.15.xt

I. INTRODUCTION

Orbital-dependent functionals in density functional theory (DFT) [1] provide seamless connection with wave function theory thus showing great promise regarding systematic and controllable improvement of the accuracy of the Kohn-Sham (KS) DFT method [2,3]. Treatment of orbital-dependent functionals in DFT requires the use of the optimized effective potential (OEP) technique for obtaining a local multiplicative Kohn-Sham potential [4–20]. In the OEP formalism, variation of the total energy functional is carried out with respect to a local multiplicative KS potential that under assumption of a fixed particle number is equivalent to the Hohenberg-Kohn variational principle [3]. Using the exchange-only energy functional the variation leads to an integral equation [4] that, in real space, possesses a unique and well-defined solution for atoms and molecules [5–7]. However, the use of finite basis sets of localized functions in the OEP method leads to a non-uniqueness of the solutions and, for the exchange-only case (xOEP), a collapse of the xOEP energies to the Hartree-Fock (HF) energies is possible [15,18]. In Ref. [18], it has been shown that a faithful solution of the OEP or xOEP equations can only be obtained with the use of a finite basis set that guarantees linear dependence of the set of products of occupied times unoccupied KS orbitals.

Currently, the popular implementation of the OEP method employs two basis sets whereby an orbital basis set is used to expand the KS orbitals and an auxiliary basis set is used for the optimized potential [13,16]. Because a straightforward use of finite basis sets in OEP leads to an ill-conditioned linear algebraic problem [8,9,19], there were suggested various ways to circumvent it by using regularization techniques [19] or by designing the auxiliary basis set in a balanced way with respect to the orbital basis set [16]. Practical utility of these approaches

however depends critically on the choice of regularization technique and its pertinent parameters [19] or on the choice of auxiliary basis set thus hard-wired into the computational scheme [16]. It is therefore desirable to formulate the OEP method in such a way that stable and accurate solutions can be found for any meaningful orbital basis set without using external conditions or parameters. Such a computational scheme will be of great practical use, because it will enable one to employ orbital-dependent density functionals on a regular basis.

In this work, we will demonstrate that with the use of the incomplete Cholesky decomposition (ICD) technique [21] the OEP equations can be solved in an arbitrary orbital basis set satisfying the condition of linear dependence of the products of occupied and virtual KS orbitals. No auxiliary basis set for expansion of the potential is employed. An arbitrarily small positive number can be chosen as the threshold δ for discriminating linearly dependent from linearly independent orbital products in the ICD method. Thus, the orbital basis set remains the only degree of freedom in setting up an OEP calculation and, with the basis sets of increased size, the xOEP total and orbital energies converge to the exact values.

II. THEORY

The OEP equations in basis set representation can be derived from direct minimization of the energy functional with respect to the local potential [18–20]. In this derivation, one necessarily starts with expanding the exchange-correlation part of the optimized potential

$$V_{xc}^{\sigma}(\mathbf{r}) = \sum_{\mu} f_{\mu\sigma}(\mathbf{r}) \tilde{w}_{\mu\sigma}, \quad (1)$$

in terms of a suitable set of expansion functions [11,13,16–19], where $\tilde{w}_{\mu\sigma}$ are the expansion coefficients and σ stands for

*m.filatov@rug.nl

spin. It is convenient to define these functions via Eq. (2) [8,11,17,20],

$$f_{\mu\sigma}(\mathbf{r}) = \int g_{\mu\sigma}(\mathbf{r}') \frac{1}{|\mathbf{r} - \mathbf{r}'|} d\mathbf{r}', \quad (2)$$

where $g_{\mu\sigma}$ are square integrable functions. Note that the expansion functions $f_{\mu\sigma}$ are not necessarily square integrable, because the local KS potential does not possess this property. The correct asymptotic behavior of the optimized potential [14,22] is fixed by requiring that the condition $\langle \phi_{\text{HOMO}} | V_{\sigma}^{xc} - \hat{V}_{\sigma}^{xc,nl} | \phi_{\text{HOMO}} \rangle = 0$ is fulfilled for the highest occupied molecular orbital (HOMO) of the system [23], where the nonlocal exchange-correlation operator is defined as $\frac{\delta E_{xc}[\{\phi_{q\sigma}\}]}{\delta \phi_{p\sigma}(\mathbf{r}')} = \hat{V}_{\sigma}^{xc,nl} \phi_{p\sigma}(\mathbf{r}')$ with $E_{xc}[\{\phi_{q\sigma}\}]$ being the orbital-dependent exchange-correlation energy (the Hartree-Fock exchange energy in the exchange-only case). Here and below we use indices i, j, \dots for occupied orbitals, a, b, \dots for virtual orbitals, and p, q, \dots for general (occupied or virtual) orbitals.

Requiring the stationarity of the total energy with respect to the local potential $V^{\sigma}(\mathbf{r}) = V_{\text{ext}}(\mathbf{r}) + \int \frac{\rho(\mathbf{r}')}{|\mathbf{r} - \mathbf{r}'|} d\mathbf{r}' + V_{xc}^{\sigma}(\mathbf{r})$, where $V_{\text{ext}}(\mathbf{r})$ is the external potential and the second term is the Coulomb potential of the electron density, is then equivalent to finding a minimum of E^{OEP} with respect to the expansion coefficients $\tilde{w}_{\mu\sigma}$. Assuming a real orbital basis and using the definition of the scalar product, $(f|g) \equiv \int f(\mathbf{r}) \frac{1}{|\mathbf{r} - \mathbf{r}'|} g(\mathbf{r}') d\mathbf{r} d\mathbf{r}'$, the minimization of E^{OEP} leads to the condition (3):

$$\begin{aligned} \frac{\partial E^{\text{OEP}}}{\partial \tilde{w}_{\mu\sigma}} &= 2 \sum_{ia} \int \phi_{i\sigma}(\mathbf{r}') [V_{\sigma}^{xc}(\mathbf{r}') - \hat{V}_{\sigma}^{xc,nl}] \\ &\quad \times \phi_{a\sigma}(\mathbf{r}') d\mathbf{r}' \frac{(g_{\mu\sigma} | \phi_{a\sigma} \phi_{i\sigma})}{\varepsilon_{a\sigma} - \varepsilon_{i\sigma}} = 0, \end{aligned} \quad (3)$$

where the KS orbitals $\phi_{p\sigma}$ are the solutions of one-electron equations $[-\frac{1}{2}\nabla^2 + V^{\sigma}(\mathbf{r})]\phi_{p\sigma}(\mathbf{r}) = \varepsilon_{p\sigma}\phi_{p\sigma}(\mathbf{r})$. Introducing the matrix $M_{\mu,ia} = (g_{\mu\sigma} | \phi_{a\sigma} \phi_{i\sigma}) / \sqrt{\varepsilon_{a\sigma} - \varepsilon_{i\sigma}}$ and the vector $w_{ia}^{nl} = \int \phi_{i\sigma}(\mathbf{r}) \hat{V}_{\sigma}^{xc,nl} \phi_{a\sigma}(\mathbf{r}) d\mathbf{r} / \sqrt{\varepsilon_{a\sigma} - \varepsilon_{i\sigma}}$, Eq. (3) can be written in matrix form as [20]

$$\nabla_{\tilde{\mathbf{w}}} E^{\text{OEP}} = 2\mathbf{M}\mathbf{M}^{\dagger}\tilde{\mathbf{w}} - 2\mathbf{M}\mathbf{w}^{nl} = 0, \quad (4)$$

where $\tilde{\mathbf{w}}$ is the vector of the expansion coefficients. Of note, Eqs. (3) and (4) are projections of the OEP equations $\sum_i^{\text{occ}} \psi[V_{\sigma}^{xc}; \mathbf{r}]\phi_i(\mathbf{r}) = 0$ [14,23] onto the set of functions $g_{\mu\sigma}$ where the aforementioned definition of the scalar product is used.

In this work, we employ the products of the occupied and virtual KS orbitals as a natural expansion basis $g_{\mu\sigma} = \phi_{j\sigma}\phi_{b\sigma} / \sqrt{\varepsilon_{b\sigma} - \varepsilon_{j\sigma}}$ in Eqs. (1) and (2) [8,12,17,20]. With this choice, the matrix elements $M_{\mu,ia}$ reduce to the two-electron integrals over the KS orbitals divided by the orbital energy differences. Because the $\phi_{j\sigma}\phi_{b\sigma}$ products do not yield potentials $f_{\mu\sigma}$ with the ‘‘monopole’’ asymptotic decay, a function that yields $-1/r$ asymptote should be included into the expansion set, for example a $g(\mathbf{r}) = \frac{1}{N}\rho(\mathbf{r})$ function that leads to the Fermi-Amaldi potential. Note that this choice of the potential expansion functions differs from the commonly adopted expansion of the OEP in terms of an auxiliary basis set [13,16,19]. Because the products of the occupied and virtual KS orbitals should be linearly dependent [18], the matrix $\mathbf{M}\mathbf{M}^{\dagger}$

becomes singular and Eq. (4) cannot be solved by matrix inversion. Following the argument by Harriman [24,25], only the linearly independent functions $f_{\mu\sigma}(\mathbf{r})$ [or $g_{\mu\sigma}(\mathbf{r})$] span the kernel space of a local multiplicative operator and can be used in the expansion of the OEP. The linearly dependent functions, which correspond to zero (or near zero, in finite accuracy arithmetics) eigenvalues of the metric matrix \mathbf{M} , span the null space and do not contribute to the expansion of a local operator [17,18,24,25]. In principle, the singular value decomposition (SVD) technique, or regularized SVD, [19] can discriminate the kernel space and the null space of a local operator. However, with the above choice of the $g_{\mu\sigma}$ basis, this makes it necessary to diagonalize a matrix of very large dimension. A more economic and numerically stable tool is provided by the ICD method [20,21,26], which is related to a partial Gram-Schmidt orthogonalization in which every vector linearly dependent with the already orthogonalized subspace of vectors is skipped [20,21,26]. ICD is capable of on-the-fly exclusion of linearly dependent eigenvectors from the expansion space of a singular positive semi-definite matrix \mathbf{A} via considering only diagonal elements of the lower triangular Cholesky matrix \mathbf{L} , $\mathbf{A} = \mathbf{L}\mathbf{L}^{\dagger}$ [20,21,26]. Provided that a diagonal matrix element is below a threshold δ , the corresponding column-vector in \mathbf{L} is neglected. The use of ICD for solving equations (4) should lead to substantial computational savings, because only a limited number ($< N_{\text{occ}} \times N_{\text{virt}}$) of the eigenvectors of \mathbf{M} contribute to the expansion of the OEP Eq. (1) [20]. In practical applications of the method, this number shows near-linear scaling with the system size [20].

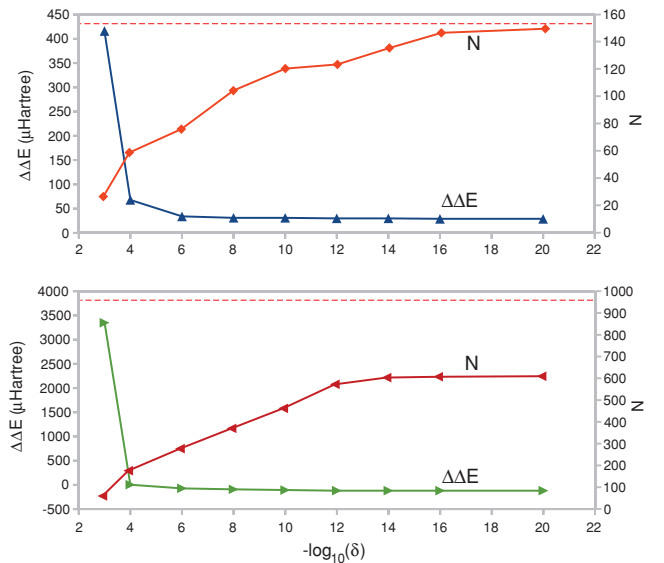


FIG. 1. (Color online) Deviations $\Delta\Delta E = [E^{\text{xOEP}}(\text{ICD}) - E^{\text{HF}}] - [E^{\text{xOEP}}(\text{NUM}) - E^{\text{HF}}(\text{NUM})]$ of the xOEP-HF energy differences for neon (upper panel) and CO (lower panel) from the numeric xOEP-HF energy differences as a function of the ICD threshold δ . Red curves (shown with diamonds in top panel and left-pointing arrows in bottom panel) give the number of expansion functions as a function of δ . The total number of totally symmetric occupied-virtual orbital products is given with dashed lines.

TABLE I. Total xOEP and HF energies of atoms and diatomic molecules (in hartree units) obtained with basis sets of varying size in comparison with the accurate numeric values.

	Basis set	xOEP(NUM) ^a	xOEP ^b	HF ^b	HF(NUM) ^c	xOEP ^d	HF ^d
Be	cc-pVTZ		-14.572 39	-14.572 87			
	cc-pVQZ		-14.572 46	-14.572 97			
	cc-pV5Z	-14.572 54	-14.572 43	-14.573 01	-14.573 02		
Ne	aug-cc-pVQZ		-128.542 51	-128.543 75		-128.542 44	-128.544 13
	aug-cc-pV5Z		-128.545 28	-128.546 79		-128.545 11	-128.546 79
	aug-cc-pV6Z	-128.545 53	-128.545 46	-128.547 06	-128.547 10	-128.545 38	-128.547 06
Mg	cc-pVTZ		-199.610 67	-199.613 35			
	cc-pVQZ		-199.611 61	-199.614 23			
	cc-pV5Z	-199.611 63	-199.611 61	-199.614 61	-199.614 64		
Ar	aug-cc-pVQZ		-526.812 16	-526.816 81			
	aug-cc-pV5Z		-526.812 29	-526.817 35			
	aug-cc-pV6Z	-526.812 34	-526.812 51	-526.817 49	-526.817 51		
Kr	aug-cc-pVTZ		-2752.041 65	-2752.052 23			
	aug-cc-pVQZ		-2752.043 58	-2752.054 72			
	aug-cc-pV5Z	-2752.043 03	-2752.043 23	-2752.054 92	-2752.054 98		
LiH	cc-pVTZ		-7.986 71	-7.986 96			
	cc-pVQZ		-7.986 99	-7.987 22			
	cc-pV5Z	-7.986 91	-7.987 97	-7.987 33			
Li ₂	cc-pVTZ		-14.870 81	-14.871 44			
	cc-pVQZ		-14.870 83	-14.871 49			
	cc-pV5Z	-14.870 76	-14.870 80	-14.871 55			
BH	aug-cc-pVQZ		-25.129 76	-25.131 34			
	aug-cc-pV5Z		-25.129 75	-25.131 56			
	aug-cc-pV6Z	-25.129 63	-25.129 67	-25.131 59			
CO	aug-cc-pVQZ		-112.784 19	-112.789 10		-112.783 55	-112.789 32
	aug-cc-pV5Z		-112.785 34	-112.790 69		-112.784 91	-112.790 71
	aug-cc-pV6Z	-112.785(3) ^e	-112.785 36	-112.790 87	-112.790 91		

^aAccurate real space values from Refs. [6] and [7].

^bThis work.

^cAccurate real space values from Refs. [30] and [31].

^dCited from Hesselmann *et al.* [16].

^eThe first unconverged digit is given in parentheses.

III. RESULTS AND DISCUSSION

The described equations were implemented in the MOL-PRO2008.2 suite of programs [27] and solutions of the OEP equations (4) in exchange-only approximation (xOEP) were obtained for a number of atoms and molecules using the standard basis sets. To guarantee linear dependence of the products of occupied and virtual KS orbitals, the correlation-consistent valence-polarized basis sets of Dunning [28] were used in an un-contracted form. First, the dependence of the xOEP atomic and molecular energies on the choice of the threshold δ in ICD was investigated. In these calculations, the largest available basis sets were used, that is cc-pV6Z or cc-pV5Z, if the former were not available.

Figure 1 shows the deviations $\Delta\Delta E = [E^{xOEP}(ICD) - E^{HF}] - [E^{xOEP}(NUM) - E^{HF}(NUM)]$ of the so-obtained xOEP-HF energy differences from the accurate numeric values for neon [6] and carbon monoxide [7] and the number of the xOEP expansion functions N as a function of the threshold δ . For large values of δ , the expansion space of the xOEP is rather small thus leading to relatively large (within a few millihartrees) deviations $\Delta\Delta E = [E^{xOEP}(ICD) - E^{HF}] - [E^{xOEP}(NUM) - E^{HF}(NUM)]$ from the target numeric xOEP-HF energy differences. Decreasing the value of δ leads

to extension of the xOEP expansion space and to a much better (within 10–100 μ hartree) agreement with the numeric xOEP energies (see also Table I). Furthermore, the deviations remain (nearly) constant when δ is varied between 10^{-6} and 10^{-20} . Beyond the latter value provided that $\epsilon \geq 0$ no noticeable variation of the xOEP energy was obtained in our calculations. Thus, the ICD procedure applied to Eq. (4) yields numerically stable solutions of the xOEP equation (4) with the energy in a very good agreement with the accurate real space methods [6,7].

For neon and CO, the obtained optimized exchange potentials are plotted in Figs. 2 and 3. Comparison with the exact exchange potential for neon [29] shows that the ICD-xOEP method yields a smooth potential that shows only tiny deviations from the exact curve. For carbon monoxide, the exact exchange potential could not be found in the literature and a comparison was not possible. However, the calculated xOEP (see Fig. 3) does not show the unphysical wiggles reported by Staroverov *et al.* [15] and is in a good agreement with the exchange potential obtained by Hesselmann *et al.* [16] with the use of auxiliary basis set.

The atomic and molecular xOEP total energies calculated with the ICD threshold $\delta = 10^{-10}$ are collected in Table I for

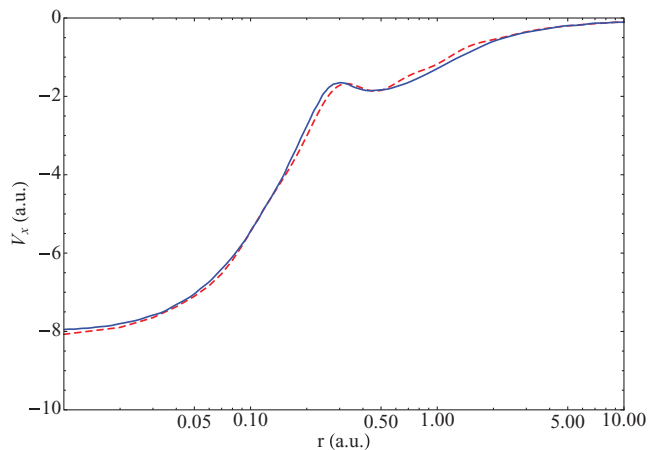


FIG. 2. (Color online) Exchange potential for Ne from the exact real space calculations (solid line) [29] and from the ICD-xOEP calculations (dashed line).

basis sets of varying size. For comparison, Table I also gives the xOEP energies obtained by Hesselmann *et al.* [16] with the use of balanced auxiliary basis sets. Note that the orbital basis sets used by Hesselmann *et al.* are augmented with a few extra basis functions and this leads to certain deviation from the total HF (and xOEP) energies obtained in the present work with the use of standard orbital basis sets. The results in Table I show that the accurate numeric xOEP energies are gradually approached with the basis sets of increasing size. Because the value of the ICD threshold δ is chosen such that it does not affect the xOEP energies, the basis set remains the only variable parameter in our xOEP calculations. Note that the xOEP energies reported in Table I are noticeably different from the HF energies. This demonstrates that, in the case of linearly dependent products

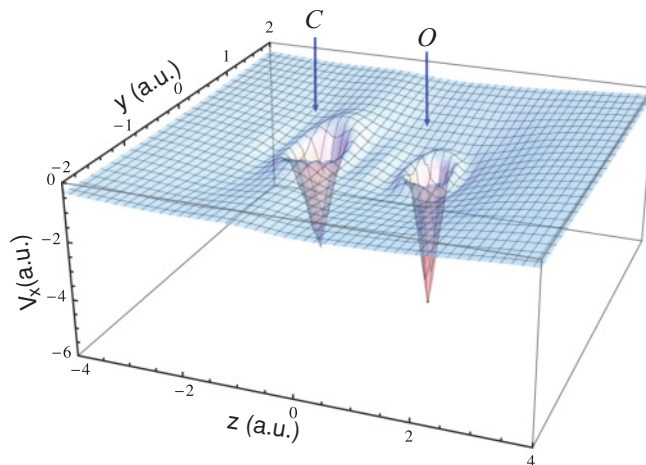


FIG. 3. (Color online) Exchange potential for CO from the ICD-xOEP calculation. The molecule is oriented along the z axis and the potential is plotted in the yz -plane. Positions of the atoms are shown with arrows.

of the occupied and virtual orbitals, there is no one-to-one mapping between densities and density matrices, i.e., many different density matrices can lead to the same density [24]. Thus these results confirm the conclusion of Görling *et al.* [18] that only the orbital basis sets that provide the linear dependence of the products of occupied and virtual KS orbitals can be used in the OEP calculations.

To demonstrate the utility of the suggested technique in the calculation of bigger molecules, a number of polyatomic molecules were calculated with the basis sets of varying size. With the increasing size of the basis set, the ICD-xOEP energies reported in Table II gradually converge to a limiting

TABLE II. Total xOEP and HF energies (in hartree units) and xOEP-HF energy differences (in millihartrees) of polyatomic molecules obtained with basis sets of varying size.

	Basis set	xOEP ^a	HF ^a	ΔE^a	xOEP ^b	HF ^b	ΔE^b
NH ₃ ^c	aug-cc-pVQZ	-56.221 58	-56.224 02	2.44			
	aug-cc-pV5Z	-56.222 26	-56.224 88	2.62			
	aug-cc-pV6Z	-56.222 28	-56.224 98	2.70			
H ₂ O ^c	cc-pVQZ	-76.063 92	-76.066 01	2.09	-76.063 61	-76.066 13	2.52
	cc-pV5Z	-76.064 96	-76.067 31	2.35	-76.064 78	-76.067 31	2.53
	cc-pV6Z	-76.065 02	-76.067 44	2.42			
C ₂ H ₂ ^c	aug-cc-pVQZ	-76.850 43	-76.854 65	4.22	-76.850 02	-76.854 72	4.70
	aug-cc-pV5Z	-76.851 14	-76.855 57	4.43	-76.850 88	-76.855 73	4.85
	aug-cc-pV6Z	-76.851 11	-76.855 68	4.57			
C ₆ H ₆ ^d	cc-pVTZ	-230.766 54	-230.779 79	13.25	-230.766 75 ^e	-230.782 76 ^e	16.01 ^e
	cc-pVQZ	-230.776 34	-230.793 37	17.03			
	cc-pV5Z	-230.778 20	-230.796 55	18.35			
C ₅ H ₅ N ^f	cc-pVTZ	-246.763 21	-246.777 39	14.18			
	cc-pVQZ	-246.774 46	-246.792 44	17.98			
	cc-pV5Z	-246.776 53	-246.795 86	19.33			

^aThis work.

^bTaken from Ref. [16] unless noted otherwise.

^cGeometry is taken from Ref. [16].

^dExperimental geometry from Ref. [33] is used.

^eTaken from Ref. [32]. Note that the HF optimized geometry was used in this work.

^fGeometry optimized with MP2/cc-pVTZ method is taken from Ref. [33].

TABLE III. xOEP and HF orbital energies of Ne, diatomic molecules, and pyridine (in hartree units). The uncontracted aug-cc-pV6Z (cc-pV5Z) basis set is used unless noted otherwise. The experimental ionization potentials are given in the last column for comparison.

System	orbital	xOEP(NUM) ^a	xOEP ^b	xOEP ^c	HF ^b	-IP(exp.)
Ne ^d	1s	-30.8200	-30.8206	-30.8200	-32.7724	
	2s	-1.7181	-1.7185	-1.7181	-1.9304	
	2p	-0.8507	-0.8507	-0.8507	-0.8504	
	3s	-0.1922	-0.1880	-0.1971	0.0475	
	3p	-0.1142	-0.1104	-0.1226	0.0464	
LiH	1 σ	-2.069(4) ^e	-2.0664		-2.4452	
	2 σ	-0.3015(9)	-0.3016		-0.3017	
	3 σ		-0.1581		-0.0039	
	1 π		-0.1269		0.0280	
Li ₂	1 σ_g	-2.01(3)	-2.0038		-2.4531	
	1 σ_u	-2.01(3)	-2.0035		-2.4528	
	2 σ_g	-0.1818(3)	-0.1818		-0.1819	
	2 σ_u		-0.1258		0.0049	
	1 π_u		-0.1136		0.0231	
BH	1 σ	-6.8126(5)	-6.8098		-7.6862	
	2 σ	-0.577(4)	-0.5767		-0.6481	
	3 σ	-0.34729(7)	-0.3471		-0.3484	
	1 π		-0.2478		0.0334	
	4 σ		-0.0892		0.0969	
CO	1 σ		-19.0666		-20.6645	-19.934 ^f
	2 σ		-10.2353		-11.3600	-10.879
	3 σ		-1.3308		-1.5215	-1.4075 ^g
	4 σ		-0.7576		-0.8045	-0.7247
	1 π		-0.6612		-0.6403	-0.6214
	5 σ		-0.5532	-0.553	-0.5549	-0.5149
	2 π		-0.2670	-0.269	0.1007	
C ₅ H ₅ N	2b ₁		-0.3735		-0.3845	-0.3730 ^h
	11a ₁		-0.3495		-0.4201	-0.3594
	1a ₂		-0.3486		-0.3482	-0.3469
	3b ₁		-0.1660		+0.0968	

^aAccurate real space values from Refs. [6] and [7].

^bThis work.

^cCited from Hesselmann *et al.* [16].

^dThe uncontracted aug-cc-pV6Z basis set augmented with a single set of diffuse functions as suggested by Hesselmann *et al.* [16] is used in this calculation.

^eThe first unconverged digit is given in parentheses.

^fThe experimental ionization potentials are taken from Ref. [34].

^gThe experimental ionization potentials are taken from Ref. [35].

^hThe experimental ionization potentials are taken from Ref. [36].

value. The $\Delta E = [E^{\text{xOEP}}(\text{ICD}) - E^{\text{HF}}]$ energy differences increase with the basis set size thus confirming the conclusion that linear dependencies of the occupied-virtual products play a crucial role for obtaining the faithful solutions of the OEP equations in finite basis sets. It is gratifying that the total xOEP energies and xOEP-HF energy differences obtained in this work with the use of large basis sets are in a good agreement with the results of alternative implementation of the finite basis set OEP method [16].

The orbital energies of Ne atom, diatomic molecules and pyridine obtained in the present xOEP calculations are collected in Table III and compared to the xOEP energies obtained in the real space calculations [6,7], to the results from Hesselmann *et al.* [16], to the Hartree-Fock orbital energies and to the available experimental ionization potentials. The orbital

energies obtained in the present xOEP calculations are in a very good agreement with the results of real space calculations which demonstrates that the exchange potentials obtained in the present work accurately reproduce the shape of the exact real space potentials (see also Fig. 2). Similar to the total xOEP energies, the orbital energies show almost no sensitivity to the choice of the ICD threshold δ which demonstrates the numeric stability of the method. It is noteworthy that the energies of frontier orbitals of pyridine are in a very good agreement with the experimental ionization potentials. Furthermore, the ordering of the 11a₁ (nitrogen lone pair) and 2b₁ (π -type) orbitals is correctly reproduced by the ICD-xOEP method whereas the HF method yields a wrong ordering of these orbital energies as can be judged from comparison with the experiment. Because the expectation values of the Fock operator calculated over the

xOEP orbitals are very close to the HF orbital energies, it is the optimized exchange potential that accounts for the correct ordering of occupied orbitals in pyridine.

IV. CONCLUSIONS

In conclusion, solutions of the exchange-only OEP method in finite basis set representation are obtained with the use of the incomplete Cholesky decomposition technique. For the first time, using the occupied-virtual orbital products as an expansion basis, numerically stable and accurate xOEP

solutions are obtained in excellent agreement with the exact real space solutions. The obtained xOEP energies show almost no dependence on the ICD threshold δ employed to discriminate the linearly independent expansion functions (kernel space of the OEP) from the linearly dependent ones (null space of the OEP) [24,25]. Thus the basis set used to expand the KS orbitals remains the only external parameter in the present implementation of the OEP method. This brings the OEP method to equal ground with the standard methods of wave function theory where the basis set size is the decisive factor for obtaining accurate results.

-
- [1] W. Kohn and L. J. Sham, *Phys. Rev.* **140**, A1133 (1965).
 [2] E. Engel and R. M. Dreizler, *J. Comput. Chem.* **20**, 31 (1999).
 [3] S. Kümmel and L. Kronik, *Rev. Mod. Phys.* **80**, 3 (2008).
 [4] R. T. Sharp and G. K. Horton, *Phys. Rev.* **90**, 317 (1953).
 [5] J. D. Talman and W. F. Shadwick, *Phys. Rev. A* **14**, 36 (1976).
 [6] E. Engel and S. H. Vosko, *Phys. Rev. A* **47**, 2800 (1993).
 [7] A. Makmal, S. Kümmel, and L. Kronik, *J. Chem. Theory Comput.* **5**, 1731 (2009).
 [8] A. Görling, *Phys. Rev. Lett.* **83**, 5459 (1999).
 [9] S. Ivanov, S. Hirata, and R. J. Bartlett, *Phys. Rev. Lett.* **83**, 5455 (1999).
 [10] S. Hirata, S. Ivanov, I. Grabowski, R. J. Bartlett, K. Burke, and J. D. Talman, *J. Chem. Phys.* **115**, 1635 (2001).
 [11] S. Ivanov, S. Hirata, and R. J. Bartlett, *J. Chem. Phys.* **116**, 1269 (2002).
 [12] R. Colle and R. K. Nesbet, *J. Phys. B* **34**, 2475 (2001).
 [13] W. Yang and Q. Wu, *Phys. Rev. Lett.* **89**, 143002 (2002).
 [14] S. Kümmel and J. P. Perdew, *Phys. Rev. B* **68**, 035103 (2003).
 [15] V. N. Staroverov, G. E. Scuseria, and E. R. Davidson, *J. Chem. Phys.* **124**, 141103 (2006).
 [16] A. Hesselmann, A. W. Götz, F. Della Sala, and A. Görling, *J. Chem. Phys.* **127**, 054102 (2007).
 [17] C. Kollmar and M. Filatov, *J. Chem. Phys.* **127**, 114104 (2007).
 [18] A. Görling, A. Hesselmann, M. Jones, and M. Levy, *J. Chem. Phys.* **128**, 104104 (2008).
 [19] T. Heaton-Burgess, F. A. Bulat, and W. Yang, *Phys. Rev. Lett.* **98**, 256401 (2007).
 [20] C. Kollmar and M. Filatov, *J. Chem. Phys.* **128**, 064101 (2008).
 [21] J. A. Meijerink and H. A. van der Vorst, *Math. Comput.* **31**, 148 (1977).
 [22] F. Della Sala and A. Görling, *Phys. Rev. Lett.* **89**, 033003 (2002).
 [23] F. Della Sala and A. Görling, *J. Chem. Phys.* **116**, 5374 (2002).
 [24] J. E. Harriman, *Phys. Rev. A* **34**, 29 (1986).
 [25] J. E. Harriman, *Phys. Rev. A* **27**, 632 (1983).
 [26] N. Beebe and J. Linderberg, *Int. J. Quantum Chem.* **12**, 683 (1977).
 [27] MOLPRO is a package of *ab initio* programs written by H.-J. Werner and P. J. Knowles, with contributions from J. Almlöf, R. D. Amos, M. J. O. Deegan, S. T. Elbert, C. Hampel, W. Meyer, K. Peterson, R. Pitzer, A. J. Stone, P. R. Taylor, R. Lindh, M. E. Mura, and T. Thorsteinsson.
 [28] T. H. Dunning Jr., *J. Chem. Phys.* **90**, 1007 (1989).
 [29] S. Kurth and S. Pittalis, in *Computational Nanoscience: Do It Yourself!*, NIC Series, Vol. 31, edited by J. Grotendorst, S. Blügel, and D. Marx (John von Neumann Institute for Computing, Jülich, 2006), pp. 299–334.
 [30] C. F. Bunge, J. A. Barrientos, A. V. Bunge, and J. A. Cogordan, *Phys. Rev. A* **46**, 3691 (1992).
 [31] F. Jensen, *Theor. Chem. Acc.* **113**, 187 (2005).
 [32] Q. Wu and W. Yang, *J. Theor. Comp. Chem.* **2**, 627 (2003).
 [33] NIST Computational Chemistry Comparison and Benchmark Database, NIST Standard Reference Database Number 101, Release 15a, April 2010, edited by Russell D. Johnson III [<http://cccbdb.nist.gov/>].
 [34] L. Pettersson, N. Wassdahl, M. Bäckström, J. E. Rubensson, and J. Nordgren, *J. Phys. B: At. Mol. Phys.* **18**, L125 (1985).
 [35] M. Nooijen and J. G. Snijders, *J. Chem. Phys.* **102**, 1681 (1994).
 [36] M. S. Moghaddam, A. D. O. Bawagan, K. H. Tan, and W. von Niessen, *Chem. Phys.* **207**, 19 (1996).